An assessment of voltammetry on disposable screen printed electrodes to predict wine chemical composition and oxygen consumption rates

Chelo Ferreira[a,d], María-Pilar Sáenz-Navajas[b], Vanesa Carrascón[a], Tormod Næs[c], Purificación Fernández-Zurbano[b], Vicente Ferreira[a*]

[a]Laboratorio de Análisis del Aroma y Enología (LAAE), Department of Analytical Chemistry, Universidad de Zaragoza, Instituto Agroalimentario de Aragón (IA2) (UNIZAR-CITA), Associate unit to Instituto de las Ciencias de la Vid y del Vino (ICVV) (UR-CSIC-GR), c/ Pedro Cerbuna 12, 50009 Zaragoza, Spain

[b]Instituto de Ciencias de la Vid y del Vino (ICVV) (Universidad de La Rioja-CSIC-Gobierno de La Rioja), Carretera de Burgos Km. 6, Finca La Grajera, 26007 Logroño, La Rioja, Spain.

[c]Nofima AS, Osloveien 1, P.O. Box 210, N-1431 Ås, Norway

[d]Instituto Universitario de Matemáticas y Aplicaciones (IUMA-UNIZAR)

*Corresponding author: vferre@unizar.es

Abstract

The present work aimed at determining the applicability of linear sweep voltammetry coupled to disposable carbon paste electrodes to predict chemical composition and wine oxygen consumption rates (OCR) by PLS-modeling of the voltammetric signal. Voltammetric signals were acquired in a set of 16 red commercial wines. Samples were extensively characterized including SO_2, antioxidant indexes, metals and polyphenols measured by HPLC. Wine OCRs were calculated by measuring oxygen consumption under controlled oxidation conditions. Chemical variables and wine OCRs were predicted from first order difference voltammogram curves by PLS-regression.

A significant number of fully validated models predicting chemical variables from voltammetric signals were obtained. This fast, cheap and easy-to-use approach presents an important potential to be used in wineries for rapid wine chemical characterization.

Key words: PLS; polyphenols; electrochemistry; oxidation; wine analysis

1. Introduction

Wine is a complex beverage consisting of hundreds of several components that experiment important changes during winemaking, many of which are definitely involved in wine quality perception (Sáenz-Navajas, Avizcuri, Ballester, Fernández-Zurbano, Ferreira, Peyron, et al., 2015). At present, wet chemistry and advanced chromatographic procedures are able to provide reliable data that allow to monitor chemical evolution of wines during winemaking and thus, can be useful tools to establish quality control programs (Ma, Bueschl, Schuhmacher, & Waterhouse, 2019; Márquez, Pérez-Navarro, Hermosín-Gutiérrez, Gómez-Alonso, Mena-Morales, García-Romero, et al., 2019). However, these methods are expensive in terms of time, personal and instrumentation resources, and therefore, are usually not affordable by small wineries. For this reason, there is a great demand for rapid, cheap and easy-to-use analytical tools that can be used to monitor wine composition and predict wine maturation processes (Kilmartin, 2016). Given the importance of wine exposure to oxygen during winemaking, modern chemistry has focused on understanding redox reactions, in which phenolic compounds are the main substrate (Singleton, Orthofer, & Lamuela-Raventós, 1998). To this concern, voltammetric approaches are presented as interesting tools for determining the content of electroactive molecules and thus monitoring oxidation-related processes involved in wine evolution (Dhroso, Laschi, Marrazza, & Mascini, 2010; Kilmartin, 2016). These methods have been applied to measure a range of antioxidants, including phenolic acids and flavonoids, ascorbic acid, SO_2 and the general resistance to oxidation (Gonzalez, Vidal, & Ugliano, 2018; José Jara-Palacios, Hernanz, Escudero-Gilete, & Heredia, 2014; Kilmartin, Zou, & Waterhouse, 2001, 2002; Martins, Oliveira, Bento, Geraldo, Lopes, De Pinho, et al., 2008; Samoticha, Jara-Palacios, Hernández-Hierro, Heredia, & Wojdyło, 2018; Ugliano, Slaghenaufi, Picariello, & Olivieri, 2020). Glass-carbon electrodes have shown to be suitable in the characterization of reducing ability of red and white wines mainly because this material minimizes ethanol interferences which dominate the signals in platinum and gold electrodes (Kilmartin, Zou, & Waterhouse, 2001, 2002; Martins, et al., 2008; Vilas-Boas, Valderrama, Fontes, Geraldo, & Bento, 2019). In recent times, disposable screen-printed graphite-based sensors are becoming more widely accessible and appear as an interesting

alternative to monitor and diagnose wine oxidation effects by direct sample measurement with no sample dilution (Dhroso, Laschi, Marrazza, & Mascini, 2010; Gonzalez, Vidal, & Ugliano, 2018; Ugliano, 2016; Ugliano, Slaghenaufi, Picariello, & Olivieri, 2020).

Even if the combination of voltammetric signals with multivariate statistical tools has been little explored, principal component analysis (Gonzalez, Vidal, & Ugliano, 2018; Ugliano, 2016) and partial least square regression modeling (Martins, et al., 2008) have been suggested to be interesting approaches to provide valuable information when monitoring wine oxidation effects or providing wine fingerprinting.

In this context, it was hypothesized that relationships between voltammogram regions and specific phenolic compounds as well as overall wine oxygen consumption rates (OCR) could be established by multivariate analysis following an untargeted voltammetric approach. Thus, the present work aimed at evaluating the applicability of linear sweep voltammetry coupled to disposable carbon paste sensors to predict chemical composition and wine oxygen consumption rates (OCR) by PLS-modeling in a set of commercial red wines.

2. Material and methods

2.1. Wine samples

A set of 16 red Spanish wines were studied. They were all purchased at a local store and were from different regions, grape varieties and vintages (detailed information is provided in Table S1 of Supporting Information).

2.2. Oxidation experiment

Oxygen consumption rates of wines were determined from data collected in an oxidation experiment consisting of five consecutive air-saturation cycles as described in Ferreira, Carrascon, Bueno, Ugliano, and Fernandez-Zurbano (2015). Air saturations were carried out by gentle shaking 500 mL of wine contained in a closed 1-liter glass bottle, then the cap was opened to allow fresh air to enter the bottle. This procedure was repeated for each saturation until a final concentration of 5.6±0.1 mg L^{-1} of dissolved oxygen was reached. Then, wine samples were incubated in the dark (25±0.5 ºC) and dissolved oxygen was monitored at least once a day with a non-destructive Nomasense oxygen analyzer (Nomacorc S.A., Thimister-Clermont, Belgium) until 90% of oxygen was consumed or during 7 days. This cycle was repeated five times.

2.3. Voltammetric measurements

Electrochemical measurements were performed with a commercial Nomasense Polyscan electrochemical analyzer (Nomacorc, Belgium) using disposable screen printed sensors. The system consisted in three sensors: working and counter electrodes both screen printed carbon paste electrodes and reference electrode consisting of an Ag/AgCl electrode. A drop of sample was loaded onto the sensor, and linear sweep voltammograms were acquired between 0 and 1200 mV at a scan rate of 100 mV s^{-1}. A total of 122 voltammetric signals for each wine in duplicate were recorded, and further worked with averaged data. A new sensor was used for each measurement. Repeatability of the measurement was tested by three consecutive measurements of the same wine.

2.4. Chemical characterization

Metals. Fe, Cu, Mn, Zn and Al were quantified by inductively coupled plasma optical emission spectroscopy (ICP-OES) with previous microwave-assisted digestion of samples as described by Gonzálvez, Armenta, and De La Guardia (2008).

Low molecular-weight polyphenols by GPC-UPLC. Compounds were analyzed in the first fraction eluting (55:45:1, ethanol:water:formic acid) from a Gel Permeation Chromatography (GPC) column filled with TSK Toyopearl gel (HW-50F) as described in Gonzalez-Hernandez, Avizcuri-Inac, Dizy, and Fernandez-Zurbano (2014). Accordingly, a total of 21 anthocyanins were quantified by UPLC-MS-DAD and 21 flavonols, 24 acids and derivatives and 11 flavanols by UPLC-MS.

Other polyphenol-related measurements. Trolox equivalent antioxidant capacity (TEAC) was measured (Rivero-Pérez, Muñiz, & González-Sanjosé, 2007) as well as total polyphenolic content by both Folin-Ciocalteu method (Singleton, Orthofer, & Lamuela-Raventós, 1998) and total polyphenol index (TPI) estimated as absorbance at 280 nm (Ribéreau-Gayon, 1970) of samples diluted 1:100 in deionized water in 1-cm-quartz cuvettes. Mean degree of polymerization was calculated as the ratio of total flavanol units (extension + terminal) to terminal units (calculated as the difference between before and after thiolysis) by acid-catalyzed degradation in the presence of toluene-α-thiol according to the method described by Labarbe, Cheynier, Brossaud, Souquet, and Moutounet (1999) but with some modifications as described by Gonzalo-Diago, Dizy, and Fernandez-Zurbano (2013). Determination of monomeric (MP), small polymeric pigments (SPP) and large polymeric pigments (LPP) was carried out as described elsewhere (Harbertson, Picciotto, & Adams, 2003). MPs were the group of compounds bleachable with bisulphite, while SPP and LPP were resistant to bisulphite bleaching. SPP did not precipitate with ovoalbumin, different to LPP. Levels of MP, SPP, and LPP were expressed as absorbance at 520 nm.

Absorbance measurements. Absorbance at 420, 520 and 620 nm of undiluted wine was measured using glass cuvettes with optical paths of 1, 2, 5 or 10 mm. Measurement which provided absorbance readings between 0.3 and 0.7 were considered as recommended by the OIV (2009a). Measurements were carried out in a Shimazdu UV-1800 (Shimadzu Corporation, Tokyo, Japan) spectrophotometer.

128 *Conventional oenological parameters.* pH was determined by Infrared Spectrometry with Fourier
129 Transformation (IRFT) with a WineScanTM FT 120 (FOSS), which was calibrated with wine
130 samples analyzed in accordance with official OIV (International Organization of Vine and Wine)
131 practices; free and total sulfur dioxide were determined by the aspiration/titration method
132 (Rankine method) recommended by the OIV.
133 *Measured Redox potential.* This parameter, which is not a truly redox potential as recently
134 discussed (Danilewicz, Tunbridge, & Kilmartin, 2019), was measured using a Pt electrode fitted
135 to a Ag/AgCl reference electrode model 50 58 from Crison (Alella, Barcelona) and a
136 microprocessor 6230N from Jenco Instruments (San Diego, CA). Measurements were recorded
137 in a glove chamber (Jacomex, France) with a level below 0.002% (v/v) of oxygen in gas phase.
138 Therefore, wine was firstly poured in a 4 mL vial where the electrode was introduced (with no
139 agitation) and measurement was recorded after 35 min. Then, the electrode was cleaned with
140 milliQ water and introduced in a solution containing equimolar amounts (0.01 M) of ferro- and
141 ferricyanide supplied by Panreac (Barcelona, Spain). This solution has a known redox potential
142 of 220 ±10 mV a 25°C (vs. Ag/AgCl(s)). If the measured redox potential was in this range, the
143 electrode was rinsed again with water and was then ready for subsequent measurements. In case
144 the measured redox potential differed more than 10 mV from the expected 220 mV value, the
145 diaphragm of the electrode was cleaned with a solution of thiourea (<6%) and HCl (<2%) (Crison,
146 Alella, Barcelona). All analyses were performed in duplicate.
147 Chemical data (average, maximum and minimum) are presented in Table S2 of Supporting
148 Information.
149 *2.5. Data treatment*
150 2.5.1. Determination of wine oxygen consumption rates
151 The oxygen consumed in the five saturation cycles was calculated for each wine (as the average
152 among three independent saturation cycles per sample) as the difference between the dissolved
153 oxygen at the beginning and at the end of each cycle. Then, the oxygen consumed for each
154 saturation was plotted against the days employed to consume the oxygen. The five points
155 (accumulated O_2 consumed at the end of each saturation, time in which saturation ended) followed

156 a straight line which was adjusted by least square regression. The ordinate at time 1 day was taken
157 as the initial oxygen consumption rate. The slope was taken as the average oxygen consumption
158 rate (Ferreira, Carrascon, Bueno, Ugliano, & Fernandez-Zurbano, 2015). Data are available in
159 Table S3 of Supporting Information.
160 2.5.2. Exploration of raw voltammetric signals
161 First derivative voltammograms allow to improve the separation between anodic waves in
162 comparison with raw voltammograms (Gonzalez, Vidal, & Ugliano, 2018). Thus, first order
163 difference voltammograms curves were calculated for all wines. Further Principal Component
164 Analysis (PCA) was calculated in order to analyze the dominating types of variability for these
165 curves and, if possible, to reduce the initial number of variables.
166 2.5.3. Modeling OCRs and chemical variables from voltammetric signals
167 The main purpose was the prediction by regressing calibration of the chemical variables from the
168 voltammograms. The general model is given by

169 $$Y = XB + F$$

170 where, for a sample size n ($n = 16$), $X_{(16,121)}$ represents the input matrix with the differences
171 between two consecutive voltammetric measurements, $Y_{(16,97)}$ the output matrix with the
172 chemical variables, $B_{(121,97)}$ is the matrix of regression coefficients and $F_{(16,97)}$ the matrix of
173 residuals.
174 Single response models are analyzed. Then, single Y - variable Partial Least Square regression
175 method is used for every chemical variable and the whole spectrum of voltammograms (X).
176 Therefore, the prediction by regressing for one single y data on X was as follows:

177 $$y_i = Xb_i + f_i,$$

178 where, $y_{i\ (16,1)}$ are the vectors that represent every one of the chemical variables $1 \leq i \leq 97$ for
179 the red wine sample set and, $b_{i\ (121,1)}$ and $f_{i\ (16,1)}$ are respectively, the vectors of regression
180 coefficients and residuals.

Firstly, the input variables X are enhanced in two ways, they have been filtered applying a 7 points window Stavizki-Golay smoothing; and, on the other hand they have been standardized to comparable noise levels. Likewise, chemical variables $y_{i;1\leq i\leq 92}$ have been standardized.

With this considerations, a first PLS model was computed. Taking the ratio between sample size and number of variables into account, variable selection has not been considered, in order to avoid the problem of overfitting. Therefore, for every single chemical variable, the whole spectrum on the X has been considerate in one PLS model. The model was validated using full cross validation. Then, those models with validated explained variance greater than 25% and presenting root mean squared error (RMSE) between the 9% and the 12% of the range were considered. Considering the size of the sample, and the number of factors that explain the main information of the $X-$variables, only models with less than or equal to four PLSs, have been considered.

All the analyses have been carried out with Unscrambler X 10.5.1, Matlab R2018a, R 4.0 and XLStat v2018.

3. Results and discussion

3.1. Voltammogram profiles

Figure 1 shows the first derivative voltammograms for the sample set. Two characteristic anodic waves with two maximal points and a minimal can be observed. The first maximal point and the minimal are around 420 mV and 600 mV, respectively. Differently, the second maximal point is around 730 mV. The derivative curve displays maximum values in the first maximal point (around 420 mV) with a derivative current reaching values of 220 nA/mV. This can be explained because red wines contain high levels of components that are rapidly involved in oxidative reactions such as anthocyanins, ortho-diphenols and triphenols of gallic acids (Table S2), which usually occur at low potential (Kilmartin, Zou, & Waterhouse, 2002) and thus can be associated with this first anodic wave. The derivative current of the second anodic wave, which corresponds to less readily oxidizable compounds (Ugliano, 2016), has been associated with vanillic or coumaric acids, the meta-diphenols on the A ring of flavonoids such as catechin, SO_2, certain amino acids and brown pigments related to oxidation reactions (Kilmartin, Zou, & Waterhouse, 2002; Makhotkina & Kilmartin, 2013).

In order to shed light on specific linkages between compounds and voltammetric signals, PLS-models have been built and discussed.

3.2. Predicting OCR from voltammetric signals

PCA was calculated with the derivative voltammetric signals. The first three PCs retain 91% (82% in validation) of original variance. This result shows that voltammetric information can be retained by three independent and non-correlated variables. Remarkably, even big efforts were invested in building PLS-models predicting chemical variables and OCRs from these three PCs, validated models could not be obtained, which could have simplified the prediction task. A possible explanation is that because we have no guarantee that the selected principal components are associated with the outcome. In fact, it is a possible drawback of PCR method (PCA + regression), where the selection of the principal components to incorporate in the model is not supervised by the outcome variable.

As detailed in the material and methods section and in a previous reference (Ferreira, Carrascon, Bueno, Ugliano, & Fernandez-Zurbano, 2015), two different OCRs were defined for red wines: the initial OCR, that corresponds to the rate of oxygen consumption during the first 24 h, and the average OCR, that refers to the average rate of consumption for the rest of the experiment. Initial OCRs are significantly faster and far more variable (0.54 – 8.22 mg O_2/L/day) than the average rates (0.365 -0.792 mg O_2/L/day). Interestingly, potentials in the first anodic wave, specifically in the 355-475 mV range (marked in green in Figure 2), present a significant negative correlation with the initial OCR ($r < -0.54$; $P < 0.05$ in all cases), while for the average OCR no significant correlation with potentials (i.e., X variables) could be established. This is a surprising result, because we had expected that higher potential signals would be related to higher contents of readily oxidizable substrates and thus to higher oxygen consumption rates. However, this result is completely equivalent to that obtained in a previous paper, in which chemical compositional parameters were just poorly positively correlated or not correlated at all with initial and average OCRs, respectively; while significant negative correlations with some chemicals were observed (Ferreira, Carrascon, Bueno, Ugliano, & Fernandez-Zurbano, 2015). In a further attempt to investigate the relationship between OCRs (initial and average) and voltammetric signals (first derivative), PLS models were calculated. Unfortunately, modeling failed to capture validated models for initial and average OCRs, thus we could not validate one of our initial hypothesis. Conversely, if a previous step consisting in the prediction of initial OCR from voltammetric potentials, but not considering the second voltammetric wave (600-1000 mV), which corresponds to less readily oxidizable compounds (Ugliano, 2016), a validated model explaining 62% of original variance for initial OCR was obtained. The model included 8 voltammetric signals with half of them displaying positive (at 20, 100, 1050 and 1130 mV: marked in orange in Figure 2) and the other half negative (300, 440, 520 and 1140 mV: marked in blue in Figure 2) relationships with initial OCR (Figure S4 of Supporting Information). Not surprisingly, the highest positive contributions to initial OCRs correspond to voltammetric signals measured at very low potentials (10 and 100 mV). It is not clear to which species can correspond signals at 10 mV, although results derived from white wines (unpublished data) suggest that it may be copper, but this result

should be further validated in future research. On its side, the signal at 100 mV could be related to the beginning of the anodic curve for ascorbic acid (Kilmartin, Zou, & Waterhouse, 2002; Makhotkina & Kilmartin, 2013). It has to be highlighted that the modeling of initial OCR from voltammetric signals omitting voltammetric signals belonging to the second anodic wave (not based on variables selection in PLS) has to be considered with caution. Given the low number of samples and high number of predicting variables, overfitting can be occurring, thus this model only establishes preliminary relationships between voltammetric signals and initial OCR. This hypothesis should be confirmed in further investigations.

3.3. Predicting chemical compositional variables from voltammetric signals

Table 1 shows the chemical variables that could be satisfactorily modeled from voltammetric signals (RMSE between the 9% and the 12% of the range) (29 out of 95). Validated models explain between 23% and 74% (average = 47%) of original variance by full-cross validation, which correspond to moderate-high correlation coefficients ranging from 0.5 to 0.9 (average = 0.7). Explained variances by calibration reach values in the range of 48-99% and corresponding to correlation coefficients between 0.7 and 0.9 (average = 0.9). Figure 3 shows the voltammetric signals (in nA of anodic current per increment of mV in the working electrode) included in models and the sign and magnitude of their coefficients following a color code. Figure 4 shows some examples of line plots representing the X-loadings corresponding to the first two PLSs (for the plots of the rest of models see Figure S5 of Supporting information). These representations are useful in the interpretation and for confirming the validity of the predictive models. These plots represent the variables (potentials of the voltammograms) that are important for predicting the variables studied such as the concentration of the compounds.

A group of flavonols (quercetin-3-*O*-glucuronide, syringetin-3-*O*-galactoside, isorhamnetin), anthocyanins (petunidin-3-*O*-glucoside, malvidin-3-*O*-glucoside, peonidin-3-*O*-(6-*O*-*p*-coumaroyl) glucoside), flavanols (catechin, epicatechin, epigallocatechin, procyanidin B1 and B2) and important chemical variables such as mean degree of polymerization of tannins and pH were satisfactorily modelled (% of explained variance > 50% by full-cross validation, i.e., correlation coefficients > 0.7). Similarly, validated models for large polymeric pigments (LPP)

and free SO_2 could explained 49% of variance in prediction (i.e., correlation coefficients of 0.7) and relatively high in calibration 63% and 92%, respectively.

Slightly poorer models with explained variance by full-cross validation higher than 23%, yet with correlation coefficients higher than 0.5, were obtained for quercetin-3-*O*-galactoside, myricetin-3-O-gluscoside, c-cinnamic acid, gallic acid ethyl ester, gallocatechin, two anthocyanins, monomeric pigments (MP), small polymeric pigments (SPP), total polyphenol index (TPI), antioxidant capacity-TEAC, absorbances at 420 and 520 nm, and for the measured redox potential. This suggesting that the related results can be presented as hypotheses to be further validated with a larger sample size.

In the case of flavonols, leaving aside quercetin, myricetin-3-galactoside and myricetin, relevant derivatives from the quantitative point of view were modelled. In the case of flavanols and anthocyanins, all the most relevant quantitatively were satisfactorily modelled. By contrast, the ability to model cinnamic, hydroxicinnamic acids and their derivatives was very poor, and only two out of 24 components could be satisfactory modelled. Most remarkably, models for predicting compositional data for metals and for absorbance at 620 nm could not be derived from the voltammetric signals.

It is interesting to note that models (Figure 3, Figure 4 and Figure S5 of Supporting Information) for flavonols, gallic acid ethyl ester, flavanols, and monomeric anthocyanins, including the overall measure of bleachable anthocyanins (MP), present positive coefficients for potentials belonging to the first anodic wave of voltammograms (mainly 140-600 mV), which is supported by the fact that these compounds are most readily oxidizable molecules of wines and thus involved in most rapid oxidative reactions (Ugliano, 2016). Differently, non-bleachable anthocyanins, named polymeric pigments (both small and large PP), can be predicted mainly from higher potentials, belonging mainly to the second wave of the first derivative of voltammograms (840-1160 mV). Among flavanols, epigallocatechin and gallocatechin show positive coefficients for lower potentials (180-250 mV) than the rest of flavanols measured (catechin, epicatechin, procyanidins B1 and B2) (270-520 mV). This is well in accordance with previous reported results, that show that gallocatechins oxidize at the surface of carbon electrodes earlier than other readily oxidizable

306 compounds, such as monomers and dimmers of (epi)catechin (Kilmartin, 2016). Remarkably is
307 that non-acylated antocyanins present similar models positively contributed by positive
308 voltametric signals at low (160-240 mV) and high (680-800 mV) potentials, while the models for
309 coumaroly anthocyanins, mainly those with higher prediction ability (delphinidin and peonidin-
310 3-*O*-(6-*O*-p-coumaroylglucosides)), show positive coefficients mainly in the first anodic wave
311 (180-480 mV), and thus they are more readily oxidizable.
312 In summary, our results suggest that the voltammetric signal in disposable carbon paste electrodes
313 is mainly the result of wine major flavonols, flavanols, anthocyanins, polymeric pigments, pH
314 and free SO_2, being poorly contributed by phenolic acids, metal cations or sulphite adducts.
315 Conversely, it can be also suggested that voltammetric information is highly multidimensional
316 and therefore can be satisfactorily used to predict many relevant chemical compositional data.

317 **Conclusions**

318 The voltammetric signals recorded from wines with disposable carbon paste electrodes are
319 extraordinarily rich in compositional information from a relatively wide range of chemical species
320 and parameters, which are suggested to be satisfactorily extracted using PLS. The best
321 performance in modelling terms was in all cases obtained from the 1^{st} derivative of the
322 voltammograms. The voltammetric signals seem to be mainly influenced by major flavonols,
323 flavanols, anthocyanins, polymeric pigments and free SO_2, all of which could be satisfactorily
324 modelled. Although oxygen consumption rates (OCR) could not be satisfactorily modelled,
325 positive correlations with voltammetric signals and satisfactory models obtained after selection
326 of variables for initial OTR (based on prior knowledge and not on PLS variable selection), allow
327 to draw the hypothesis that OCRs have a potential of being satisfactorily predicted and thus
328 voltammetry could be also a suitable rapid tool for predicting OCR.
329 The results presented in this work suggest that disposable carbon paste sensors measuring
330 voltammetric signals and coupled to PLS-modeling have an important potential to be used in
331 wineries for rapid, cheap and easy-to-use approach for wine chemical characterization and
332 oxidation-related control. It is important to emphasize that the number of samples is quite low

and also that only the best models are selected for presentation in Table 1. Therefore the present work is a feasibility study and models must be validated on new data to confirm the results.

Acknowledgements

Funded by the Spanish Ministry of Economy and Competitiveness (MINECO) (projects RTC-2016-4935-2, AGL-2017-87373-C3-1-R and AGL-2017-87373-C3-3-R). MPSN acknowledges the Spanish National Research Agency, the Ministry of Science, Innovation, and Universities and the European Social Fund for her postdoctoral fellowship: Ramón y Cajal Program (RYC2019-027995-I/AEI/10.13039/501100011033).

C.F acknowledges the support and hospitality of institute NOFIMA (Norway), especially Tormod Næs research team. LAAE acknowledges the continuous support of Diputación General de Aragón (T53) and European Social Fund. The authors would like to thank Dr. Paul Kilmartin for his advice and discussions on voltammetric data.

Appendix A. Supplementary information

Supplementary information associated with this article can be found online at Supplementary data to this article can be found online at https://doi.org/xx.xxx/food.chem

References

Danilewicz, J. C., Tunbridge, P., & Kilmartin, P. A. (2019). Wine Reduction Potentials: Are These Measured Values Really Reduction Potentials? *Journal of Agricultural and Food Chemistry, 67*(15), 4145-4153.

Dhroso, A., Laschi, S., Marrazza, G., & Mascini, M. (2010). A fast electrochemical technique for characterization of phenolic content in wine. *Analytical Letters, 43*(7), 1190-1198.

Ferreira, V., Carrascon, V., Bueno, M., Ugliano, M., & Fernandez-Zurbano, P. (2015). Oxygen Consumption by Red Wines. Part I: Consumption Rates, Relationship with Chemical Composition, and Role of SO<inf>2</inf>. *Journal of Agricultural and Food Chemistry, 63*(51), 10928-10937.

Gonzalez-Hernandez, M., Avizcuri-Inac, J. M., Dizy, M., & Fernandez-Zurbano, P. (2014). Ultra Performance Liquid Chromatography Coupled to Ultraviolet-Vis and Mass Spectrometry Detector for Screening of Organic Acids and Polyphenols in Red Wine In High-Performance Liquid Chromatography (HPLC): . In Y. Zuo (Ed.), *Principles, Practices and Procedures;*). New York: Nova Science Pub Inc.

Gonzalez, A., Vidal, S., & Ugliano, M. (2018). Untargeted voltammetric approaches for characterization of oxidation patterns in white wines. *Food Chemistry, 269*, 1-8.

Gonzalo-Diago, A., Dizy, M., & Fernandez-Zurbano, P. (2013). Taste and Mouthfeel Properties of Red Wines Proanthocyanidins and Their Relation to the Chemical Composition. *Journal of Agricultural and Food Chemistry, 61*(37), 8861-8870.

Gonzálvez, A., Armenta, S., & De La Guardia, M. (2008). Trace elemental composition of curry by inductively coupled plasma optical emission spectrometry (ICP-OES). *Food Additives and Contaminants: Part B Surveillance, 1*(2), 114-121.

Harbertson, J., Picciotto, E., & Adams, D. (2003). Measurement of polymeric pigments in grape berry extracts and wines using a protein precipitation assay combined with bisulfite bleaching. *American Journal of Enology and Viticulture, 54*(4), 301-306.

José Jara-Palacios, M., Hernanz, D., Escudero-Gilete, M. L., & Heredia, F. J. (2014). Antioxidant potential of white grape pomaces: Phenolic composition and antioxidant capacity measured by spectrophotometric and cyclic voltammetry methods. *Food Research International, 66*, 150-157.

Kilmartin, P. A. (2016). Electrochemistry applied to the analysis of wine: A mini-review. *Electrochemistry Communications, 67*, 39-42.

Kilmartin, P. A., Zou, H., & Waterhouse, A. L. (2001). A cyclic voltammetry method suitable for characterizing antioxidant properties of wine and wine phenolics. *Journal of Agricultural and Food Chemistry, 49*(4), 1957-1965.

Kilmartin, P. A., Zou, H., & Waterhouse, A. L. (2002). Correlation of wine phenolic composition versus cyclic voltammetry response. *American Journal of Enology and Viticulture, 53*(4), 294-302.

Labarbe, B., Cheynier, V., Brossaud, F., Souquet, J. M., & Moutounet, M. (1999). Quantitative fractionation of grape proanthocyanidins according to their degree of polymerization. *Journal of Agricultural and Food Chemistry, 47*(7), 2719-2723.

Ma, L., Bueschl, C., Schuhmacher, R., & Waterhouse, A. L. (2019). Tracing oxidation reaction pathways in wine using 13 C isotopolog patterns and a putative compound database. *Analytica Chimica Acta, 1054*, 74-83.

Makhotkina, O., & Kilmartin, P. A. (2013). Electrochemical oxidation of wine polyphenols in the presence of sulfur dioxide. *Journal of Agricultural and Food Chemistry, 61*(23), 5573-5581.

Márquez, K., Pérez-Navarro, J., Hermosín-Gutiérrez, I., Gómez-Alonso, S., Mena-Morales, A., García-Romero, E., & Contreras, D. (2019). Systematic study of hydroxyl radical production in white wines as a function of chemical composition. *Food Chemistry, 288*, 377-385.

Martins, R. C., Oliveira, R., Bento, F., Geraldo, D., Lopes, V. V., De Pinho, P. G., Oliveira, C. M., & Silva Ferreira, A. C. (2008). Oxidation management of white wines using cyclic voltammetry and multivariate process monitoring. *Journal of Agricultural and Food Chemistry, 56*(24), 12092-12098.

Rivero-Pérez, M. D., Muñiz, P., & González-Sanjosé, M. L. (2007). Antioxidant profile of red wines evaluated by total antioxidant capacity, scavenger activity, and biomarkers of oxidative stress methodologies. *Journal of Agricultural and Food Chemistry, 55*(14), 5476-5483.

Sáenz-Navajas, M. P., Avizcuri, J. M., Ballester, J., Fernández-Zurbano, P., Ferreira, V., Peyron, D., & Valentin, D. (2015). Sensory-active compounds influencing wine experts' and consumers' perception of red wine intrinsic quality. *LWT - Food Science and Technology, 60*, 400-411.

Samoticha, J., Jara-Palacios, M. J., Hernández-Hierro, J. M., Heredia, F. J., & Wojdyło, A. (2018). Phenolic compounds and antioxidant activity of twelve grape cultivars measured by chemical and electrochemical methods. *European Food Research and Technology, 244*(11), 1933-1943.

Singleton, V. L., Orthofer, R., & Lamuela-Raventós, R. M. (1998). Analysis of total phenols and other oxidation substrates and antioxidants by means of folin-ciocalteu reagent. In *Methods in Enzymology*, vol. 299 (pp. 152-178).

419 Ugliano, M. (2016). Rapid fingerprinting of white wine oxidizable fraction and classification of
420 white wines using disposable screen printed sensors and derivative voltammetry. *Food*
421 *Chemistry, 212*, 837-843.
422 Ugliano, M., Slaghenaufi, D., Picariello, L., & Olivieri, G. (2020). Oxygen and SO2 consumption of
423 different enological tannins in relationship to their chemical and electrochemical
424 Characteristics. *Journal of Agricultural and Food Chemistry, 68*(47), 13418-13425.
425 Vilas-Boas, Â., Valderrama, P., Fontes, N., Geraldo, D., & Bento, F. (2019). Evaluation of total
426 polyphenol content of wines by means of voltammetric techniques: Cyclic voltammetry
427 vs differential pulse voltammetry. *Food Chemistry, 276*, 719-725

Figure captions

Figure 1. First derivative voltammograms for sixteen Spanish red wines.

Figure 2. First derivative voltammograms of wines with highest and lowest oxygen consumption rates among red wines. Regions marked in green present significant correlations with OCR. In orange voltammetric signals with positive and in blue with negative coefficients in the models predicting OCRs

Figure 3. Maps with coefficients of variables included in validated PLS-models predicting chemical variables from voltammetric signals for red wines.

Figure 4. The X-loadings for the two first PLS components based on the PLS model for a) quercetin-3-*O*-galactoside, b) quercetin-3-glucoronide, c) catechin, d) epigallocatechin, e) malvidin-3-*O*-glucoside, and petunidin-3-*O*-glucoside. The red line represents the first PLS and the blue the second PLS line the second

Supplementary Information for

An assessment of voltammetry on disposable screen printed electrodes to predict wine chemical composition and oxygen consumption rates

Chelo Ferreira[a,d], María-Pilar Sáenz-Navajas[a]*, Vanesa Carrascón[a], Tormod Næs[b], Purificación Fernández-Zurbano[c], Vicente Ferreira[a]

[a]Laboratorio de Análisis del Aroma y Enología (LAAE), Department of Analytical Chemistry, Universidad de Zaragoza, Instituto Agroalimentario de Aragón (IA2) (UNIZAR-CITA), Associate unit to Instituto de las Ciencias de la Vid y del Vino (ICVV) (UR-CSIC-GR), c/ Pedro Cerbuna 12, 50009 Zaragoza, Spain

[b]Nofima AS, Osloveien 1, P.O. Box 210, N-1431Ås, Norway

[c]Instituto de Ciencias de la Vid y del Vino (ICVV) (CSIC-Gobierno de La Rioja- Universidad de La Rioja), Carretera de Burgos Km. 6, Finca La Grajera, 26007 Logroño, La Rioja, Spain.

[d]Instituto Universitario de Matemáticas y Aplicaciones (IUMA-UNIZAR)

*Corresponding author: mpsaenz@icvv.es

Table of Contents

Table S1. Information of wines employed in the study.

Table S2. Chemical characterization of the 16 red wines studied (data expressed as micrograms per liter, otherwise it is specified). Compounds marked in red were satisfactorily modeled from voltammograms.

Table S3. Initial and average oxygen consumption rates for red wines (OCR) expressed as mg O_2/L/day (average of three independent replicates).

Figure S4. Map with coefficients of variables included in validated PLS-models predicting initial OTR from voltammetric signals.

Figure S5. The X-loadings for the two first PLS components based on the PLS model for a) flavonols, b) acids and derivatives, c) flavanols, d) anthocyanins, e) anthocyanic pigments, and f) other parameters

Table S1. Information of wines employed in the study.

set of wine	code	vintage	grape variety	origin	time in barrel (months)	% ethanol (v/v)	pH	TPI (a.u.)
red wines	R1	2008	Tempranillo	Ribera del Duero	18	14.1	3.9	53.5
	R2	2007	Tempranillo	Rioja	>6	13.5	3.8	55.1
	R3	2008	Garnacha	Campo de Borja	>6	13.5	3.5	61.9
	R4	2010	Garnacha	Campo de Borja	>6	14.5	3.5	86.5
	R5	2012	Tempranillo	Rioja	0	13	3.9	48.2
	R6	2012	Garnacha, Tempranillo	Calatayud	0	14	3.8	62.2
	R7	2012	Tempranillo	Ribera del Duero	6	13.5	3.7	60.8
	R8	2012	Syrah	Vinos de la tierra de Castilla	0	14.5	3.7	69.0
	R9	2010	Tempranillo, Mazuelo, Graciano	Rioja	3	13.5	3.5	52.2
	R10	2011	Garnacha	Campo de Borja	>6	15	3.4	57.9
	R11	2010	Tempranillo	Toro	14	14.5	3.9	66.0
	R12	2008	Garnacha	Campo de Borja	10	15	3.5	72.3
	R13	2009	Syrah, Merlot, Cabernet Sauvignon	Cariñena	>6	14.5	3.6	62.3
	R14	2010	Garnacha	Campo de Borja	>6	15.5	3.4	57.9
	R15	2012	Cabernet Sauvignon, Merlot	Somontano	0	13.5	3.5	60.9
	R16	2012	Tempranillo	Rioja	6	13.5	3.8	53.4

Table S2. Chemical characterization of the 16 red wines studied (data expressed as micrograms per liter, otherwise it is specified). Compounds marked in red were satisfactorily modelled from voltammograms.

Compounds	average	max	min
Flavonols			
quercetin-3-galactoside	1.22	3.69	0.51
quercetin-3-glucoside	1.57	14.58	0.00
quercetin-3-glucuronide	8.86	19.99	3.00
quercetin-3-rutinoside	0.04	0.62	0.00
quercetin	3.05	5.88	1.75
kaempferol-3-glucoside	0.16	1.36	0.00
kaempferol-3-galactoside	0.07	0.31	0.00
kaempferol-3-glucuronide	0.06	0.21	0.00
kaempferol-3-rutinoside	0.30	0.52	0.15
kaempferol	0.96	1.57	0.00
syringetin-3-galactoside	1.47	3.13	0.55
myricetin-3-galactoside	2.90	12.60	1.19
myricetin-3-glucoside	3.45	13.43	1.20
myricetin-3-glucuronide	1.57	1.90	1.35
myricetin-3-rutinoside	1.18	1.21	1.17
myricetin	4.39	7.36	2.48
isorhamnetin -3-glucoside	0.48	4.48	0.00
isorhamnetin -3-galactoside	0.11	0.22	0.00
isorhamnetin -3-glucuronide	0.07	0.14	0.00
isorhamnetin -3-rutinoside	0.14	0.22	0.00
isorhamnetin	4.70	7.67	2.74
Acids and derivatives			
gallic acid	35.14	56.12	22.30
protocatechuic acid	1.10	2.33	0.61
c-caftaric acid	3.13	9.75	0.00
t-caftaric acid	57.79	120.89	21.56
3,4-hydroxyphenylacetic acid	0.31	2.01	0.00
cutaric acid	4.37	6.60	2.72
vanillic acid	0.35	0.54	0.23
caffeic acid	5.79	12.72	1.44
syringic acid	1.06	1.73	0.70
c-coumaric-acid	0.82	0.94	0.00
coumaric acid	1.63	4.26	0.98
c-cinnamic acid	7.73	10.10	5.42
trans-cinnamic acid	17.48	22.10	12.26
protocatechuic acid ethyl ester	0.19	0.47	0.00
caffeic acid ethyl ester	0.79	1.33	0.00
ferulic acid ethyl ester	0.00	0.00	0.00
syringic acid ethyl ester	0.00	0.00	0.00
ellagic acid	24.78	30.58	19.80
gallic acid ethyl ester	2.23	4.06	1.35
coumaric acid ethyl ester	0.52	0.94	0.00
c-aconitic acid	1.99	2.48	1.56
t-aconitic acid	1.45	3.50	0.00
c-ferulic acid	0.36	1.48	0.00
t-ferulic acid	0.34	1.60	0.00
Flavanols			
procyanidin B1	10.75	27.66	3.27
epigallocatechin	6.26	10.28	3.88
catechin	7.48	23.04	3.56
procyanidin B2	5.13	16.44	1.89
epicatechin	5.10	18.88	2.72
epigallocatechin gallate	2.57	3.74	1.73
catechin gallate	0.05	0.40	0.00
epicatechin gallate	0.95	1.26	0.00
procyanidin A2	0.85	1.97	0.00
gallocatechin	3.05	4.25	1.33
gallocatechin gallate	0.82	2.99	0.00
Anthocyanins			
B-type vitisin of delphinidin-3-*O*-glucoside	0.05	0.08	0.02
cyanidin-3-glucoside	0.10	0.23	0.05
petunidin-3-glucoside	1.98	9.48	0.03
peonidin-3-glucoside	0.28	0.74	0.03
malvidin-3-glucoside	17.13	75.60	0.16
delphinidin-3-*O*-(6-*O*-acetyl) glucoside	0.02	0.02	0.02
vitisin A	0.21	0.59	0.03

Table S2 contd.

Compounds	average	max	min
B-Type vitisin of malvidin-3-oglucoside	0.02	0.02	0.02
petunidin-3-*O*-(6-*O*-acetyl) glucoside	0.02	0.03	0.02
malvidin-3-*O*-glucoside-8-ethyl-(epi)catechin	0.06	0.25	0.02
delphinidin-3-*O*-(6-*O*-p-coumaroyl) glucoside	0.80	5.02	0.02
malvidin-3-*O*-(6-*O*-acetyl) glucoside	0.03	0.05	0.02
A-type vitisin of malvidin-3-O-(6-O-p-coumaroyl)glucoside	0.02	0.02	0.02
petunidin-3-*O*-(6-*O*-p-coumaroyl) glucoside	0.05	0.17	0.02
malvidin-3-*O*-(6-*O*-p-coumaroyl) glucoside	0.03	0.07	0.02
peonidin-3-*O*-(6-*O*-p-coumaroyl) glucoside	0.04	0.14	0.02
malvidin-3-*O*-glucoside-4-vinylphenol	0.03	0.05	0.02
malvidin-3-*O*-acetylglucoside-4-vinylphenol	0.02	0.02	0.02
Polyphenol-related measurements			
mean degree of polimerization of flavanols (mDP)	1.80	2.08	1.54
small polymeric pigments (SPP)	0.54	0.76	0.26
large polymeric pigments (LPP)	0.42	0.69	0.14
monomeric pigments (MP)	0.42	0.91	0.25
proanthocyanidins (mg/L, expressed as equivalents of catechin)	840	1371	304
protein-precipitable flavanols (mg/L, expressed as equivalents of tannic acid)	1.32	2.26	0.48
antioxidant capacity-TEAC (Mm, expressed as equivalents of Trolox)	40.47	63.50	29.53
antioxidant capacity-Folin (mg/L, expressed as equivalents of gallic acid)	2883	3354	2353
free SO_2 (mg L^{-1})	17.84	36.54	4.53
total SO_2 total (mg L^{-1})	48.30	73.60	14.40
Color			
Abs 420 nm (au)	4.32	5.72	2.68
Abs 520 nm (au)	5.46	7.72	3.72
Abs 620 nm (au)	1.75	4.24	1.11
Metals			
Al	0.14	1.17	0.00
Cu	0.26	0.68	0.17
Fe	2.44	4.07	1.46
Mn	1.15	2.57	0.54
Zn	0.63	1.33	0.22
Redox Potential (mV)	14.50	59.00	-10.00

Table S3. Initial and average oxygen consumption rates for red wines (OCR) expressed as mg O_2/L/day (average of three independent replicates)

code	Initial OCR	Average OCR
R1	1.73±0.56	0.60±0.03
R2	7.70±0.49	0.59±0.03
R3	2.82±0.54	0.58±0.02
R4	1.80±0.07	0.68±0.00
R5	7.89±0.40	0.66±0.02
R6	0.54±0.40	0.65±0.02
R7	1.62±0.65	0.52±0.03
R8	0.89±0.26	0.61±0.02
R9	8.22±0.56	0.40±0.03
R10	6.12±0.49	0.47±0.02
R11	5.73±0.35	0.79±0.03
R12	5.43±0.30	0.72±0.02
R13	2.52±0.62	0.55±0.03
R14	3.45±0.31	0.37±0.01
R15	0.80±0.15	0.54±0.01
R16	2.39±0.51	1.27±0.04

Figure S4. Map with coefficients of variables included in validated PLS-model predicting initial oxygen consumption rate (initial OCR) from voltammetric signals.

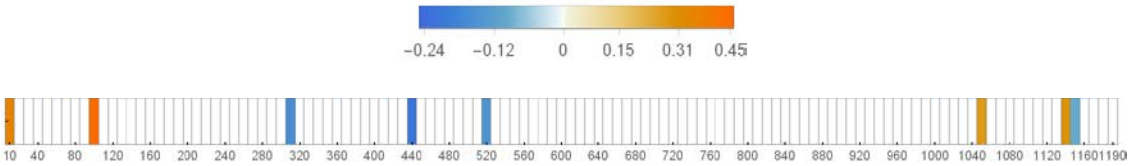

Figure S5.

a) FLAVONOLS

a. syringetin-3-galactoside

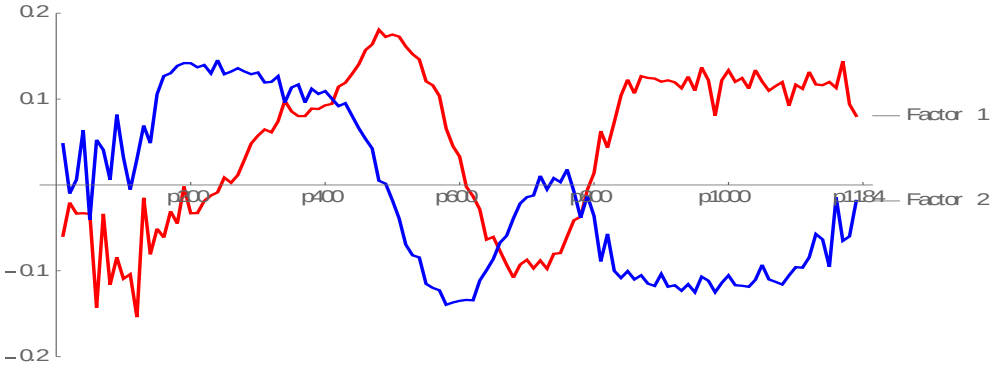

b. myricetin-3-glucoside

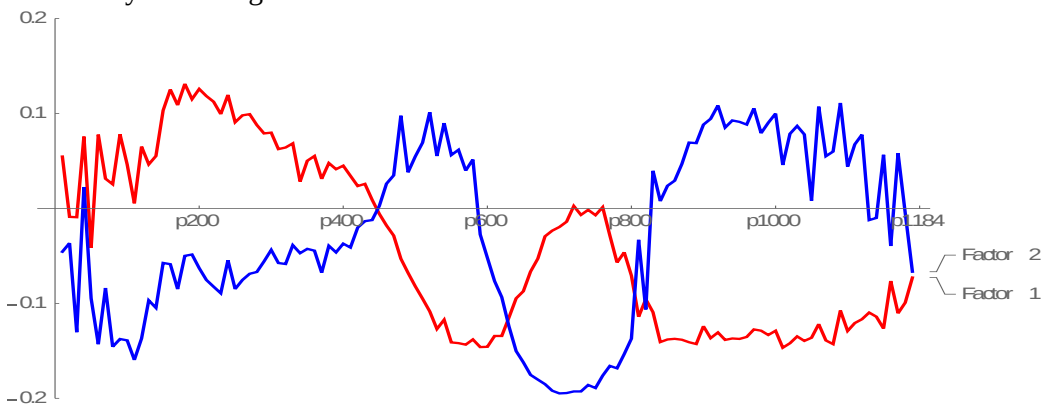

c. isorhamnetin

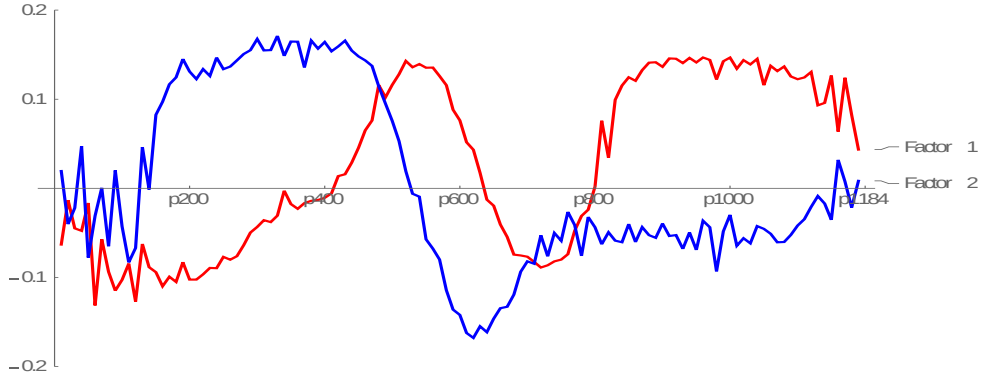

b) ACIDS AND DERIVATIVES

a. c-cinnamic acid

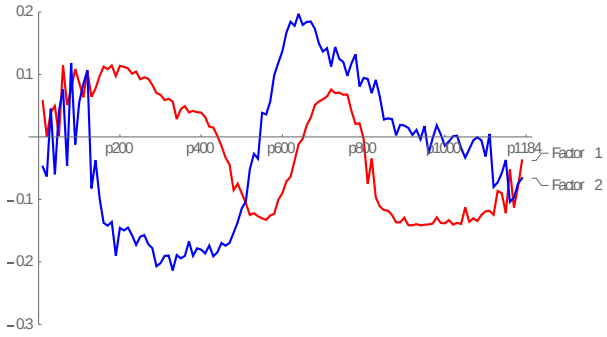

b. gallic acid ethyl ester

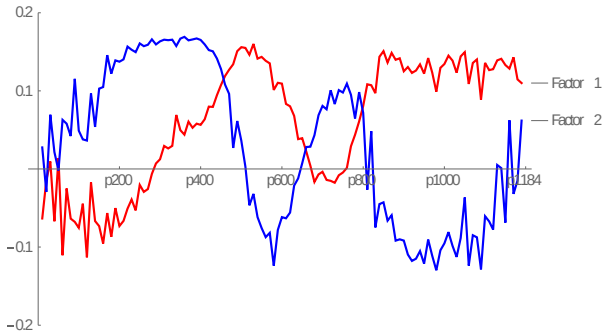

c) FLAVANOLS

a. epicatechin

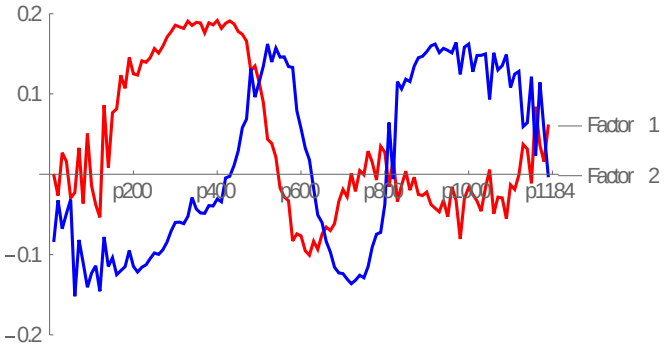

b. gallocatechin

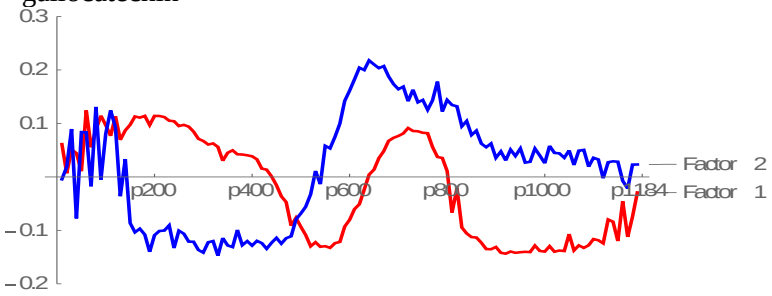

c. procyanidin B1

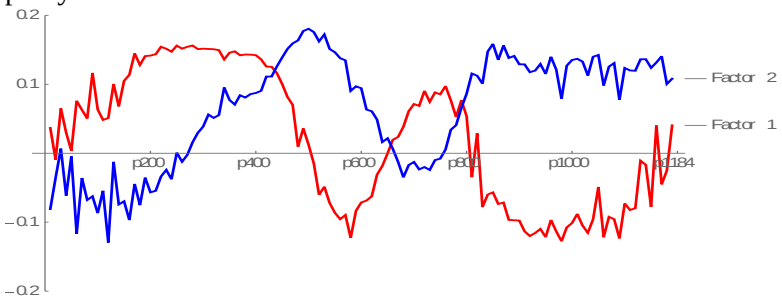

d. procyanidin B2

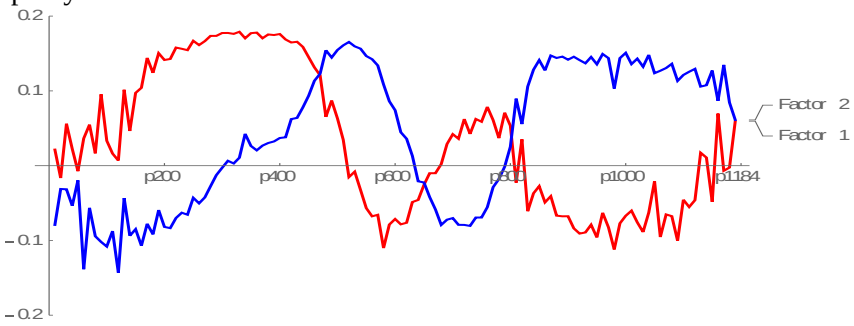

d) ANTHOCYANINS

a. malvidin-3-O-glucoside-8-ethyl-(epi)catechin

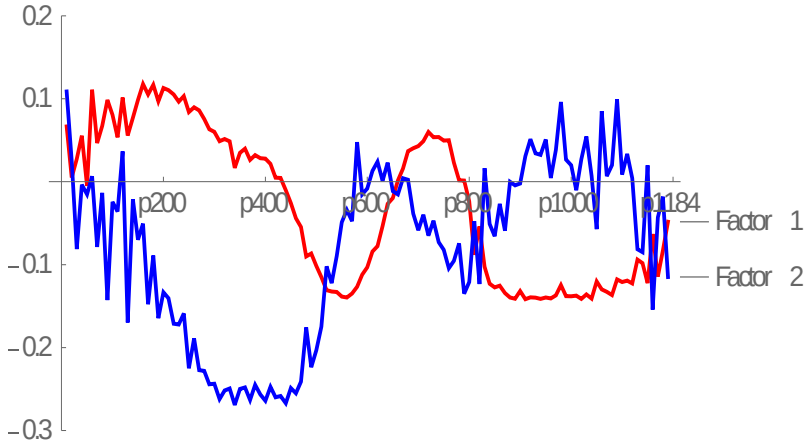

b. malvidin-3-O-(6-O-acetyl)glucoside

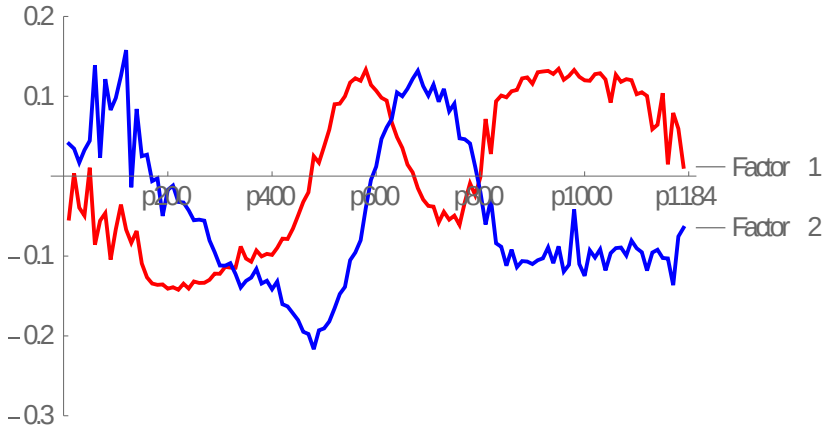

c. peonidin-3-O-(6-O-p-coumaroyl)glucoside

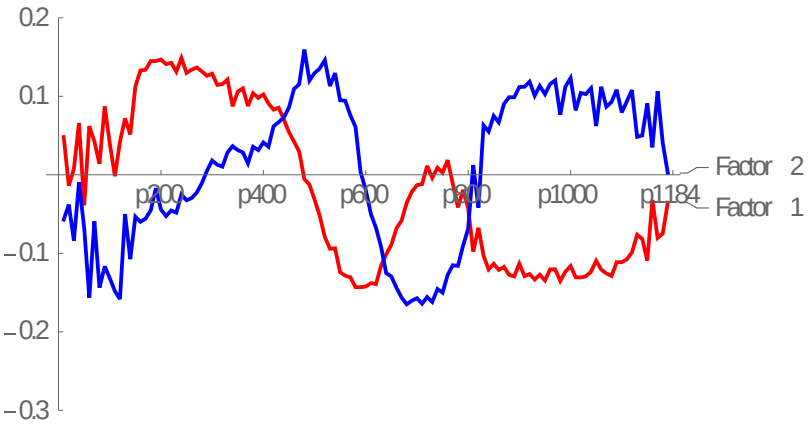

e) ANTHOCYANIC PIGMENTS

a. SPP

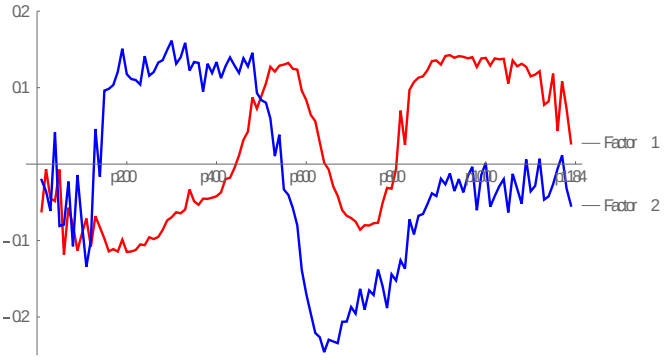

b. LPP

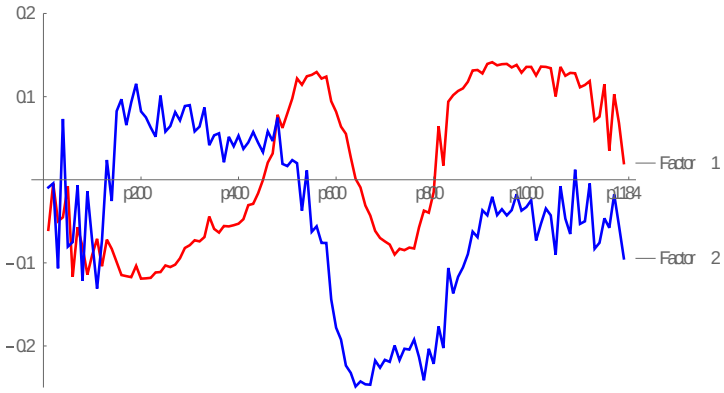

c. MP

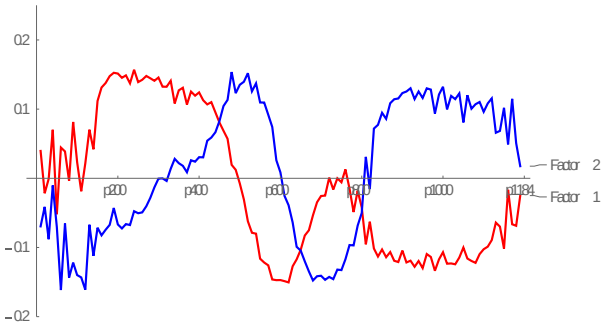

f) OTHER PARAMETERS

a. mDP

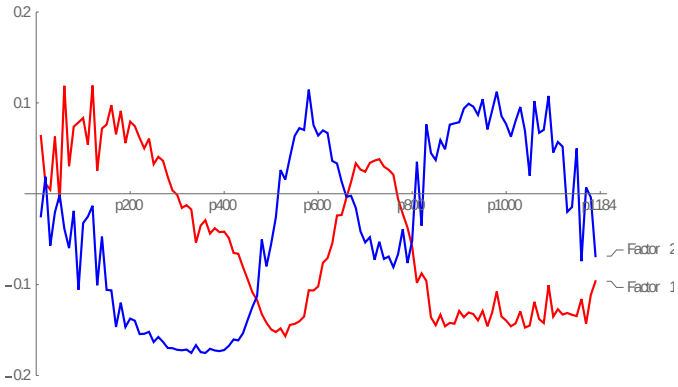

b. TPI

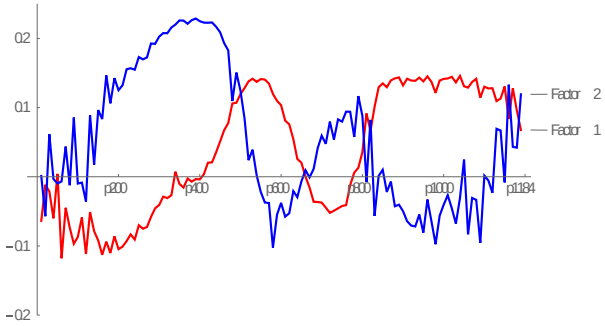

c. TEAC

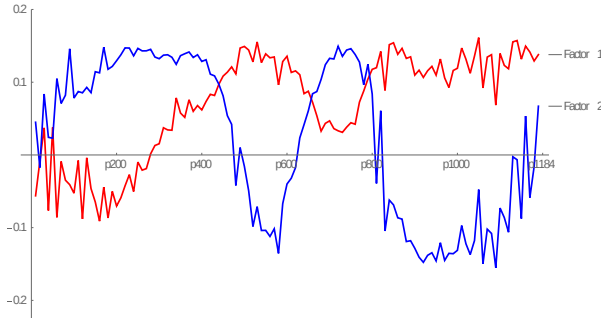

d. absorbance at 420nm

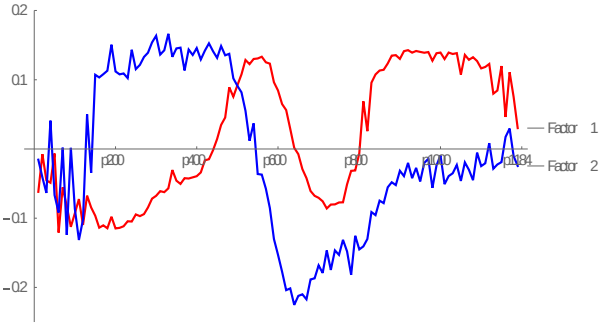

e. absorbance at 520nm

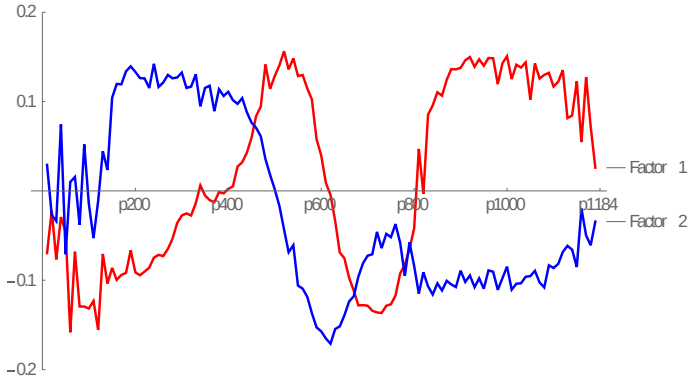

f. pH

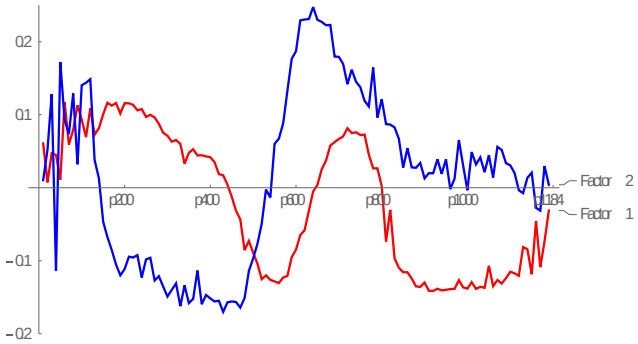

g. redox potential

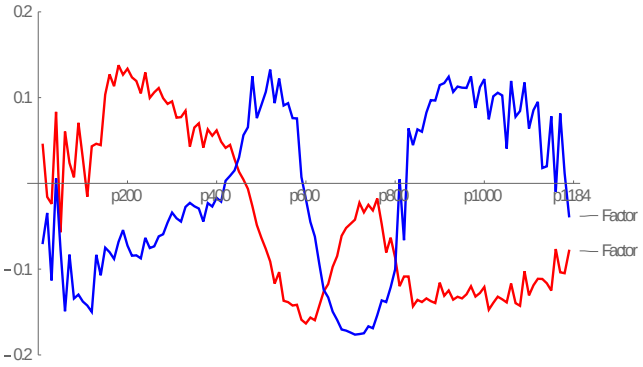

h. free SO_2

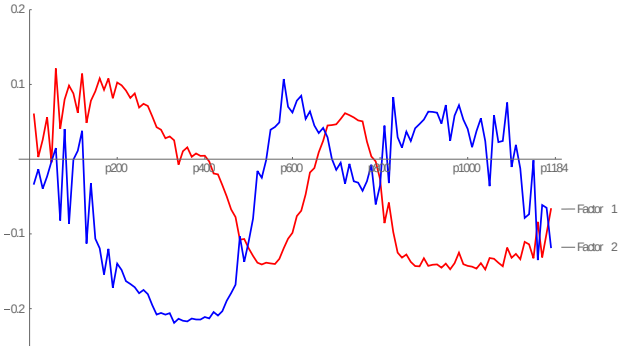

Table 1. Variables successfully modeled in the set of red wines (n=16) from voltammetric signals by PLS regression, % of explained variance by full cross validation (and the % of explained variance), the number of PLSs included in each model and the root mean squared error of prediction.

	variable	*% explained variance P (number of PLSs) [% explained variance C]*	*RMSE*[1]
flavonols	quercetin-3-galactoside	41% (2) [75%]	0.48
	quercetin-3-glucuronide	58% (2) [76%]	0.47
	syringetin-3-galactoside	74% (2) [88%]	0.34
	myricetin-3-glucoside	44% (3) [83%]	0.39
	isorhamnetin	52% (2) [79%]	0.44
acids and derivatives	*c*-cinnamic acid	48% (1) [57%]	0.63
	gallic acid ethyl ester	38% (2) [66%]	0.56
flavanols	catechin	64% (4) [93%]	0.25
	epicatechin	57% (4) [94%]	0.24
	epigallocatechin	55% (1) [69%]	0.54
	gallocatechin	37% (1) [57%]	0.63
	procyanidin B1	56% (2) [76%]	0.48
	procyanidin B2	63% (1) [80%]	0.43
anthocyanins	petunidin-3-*O*-glucoside	60% (4) [99%]	0.09
	malvidin-3-*O*-glucoside	65% (4) [99%]	0.08
	malvidin-3-*O*-glucoside-8-ethyl-(epi)catechin	43% (4) [99%]	0.11
	malvidin-3-*O*-(6-*O*-*p*-coumaroyl)glucoside	41% (1) [61%]	0.60
	peonidin-3-*O*-(6-*O*-*p*-coumaroyl)glucoside	51% (2) [85%]	0.37
polyphenol-related measurements	small polymeric pigments (SPP)	30% (1) [50%]	0.69
	large polymeric pigments (LPP)	49% (1) [63%]	0.59
	monomeric pigments (MP)	23% (3) [88%]	0.51
	mean degree of polymerization (mDP)	53% (1) [88%]	0.17
	total polyphenol index (TPI)	26% (1) [48%]	0.69
	antioxidant capacity-TEAC	29% (2) [65%]	0.57
color	absorbance at 420nm	38% (1) [56%]	0.64
	absorbance at 520nm	38% (2) [72%]	0.51
other parameters	pH	51% (1) [61%]	0.61
	redox potential	28% (2) [67%]	0.56
	free SO_2	49% (4) [92%]	0.27

[1]RMSE is given in z-units for a normal distribution. Given that 99.7% of normal values are between z=-3 and z=3, a RMSE of 0.6 represents around 10% of the range.

Figure 1

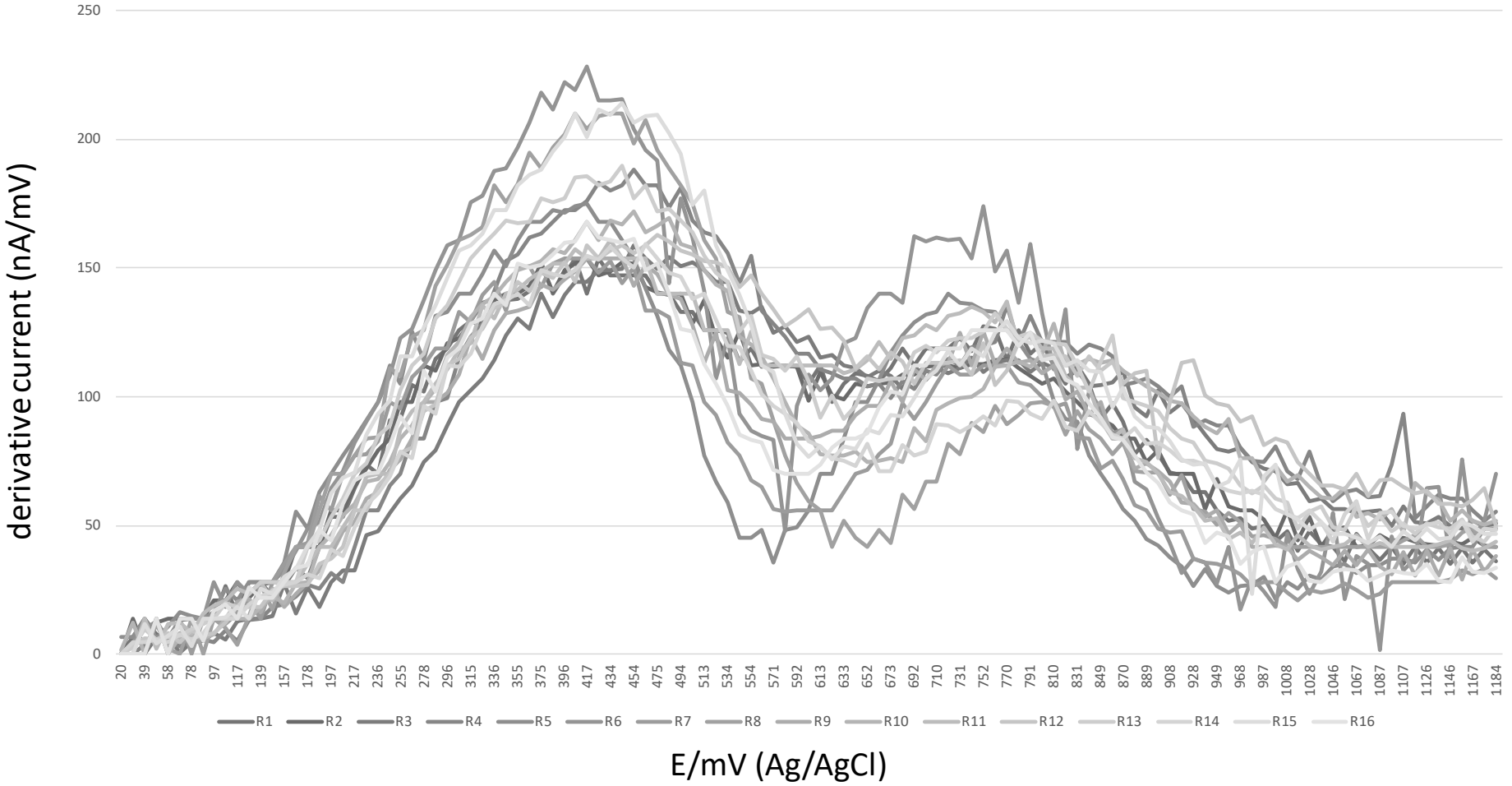
250
200
150
100
50
0
derivative current (nA/mV)
20 39 58 78 97 117 139 157 178 197 217 236 255 278 296 315 336 355 375 396 417 434 454 475 494 513 534 554 571 592 613 633 652 673 692 710 731 752 770 791 810 831 849 870 889 908 928 949 968 987 1008 1028 1046 1067 1087 1107 1126 1146 1167 1184
R1 R2 R3 R4 R5 R6 R7 R8 R9 R10 R11 R12 R13 R14 R15 R16
E/mV (Ag/AgCl)

Figure 2

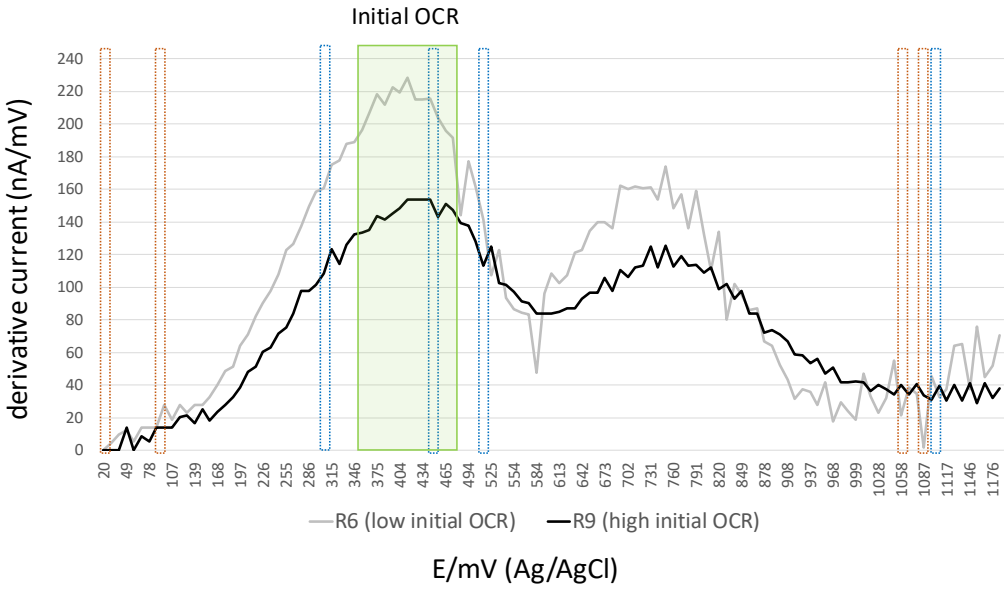
Initial OCR
derivative current (nA/mV)
240
220
200
180
160
140
120
100
80
60
40
20
0
20 49 78 107 139 168 197 226 255 286 315 346 375 404 434 465 494 525 554 584 613 642 673 702 731 760 791 820 849 878 908 937 968 999 1028 1058 1087 1117 1146 1176
R6 (low initial OCR)
R9 (high initial OCR)
E/mV (Ag/AgCl)

Figure 3

a)

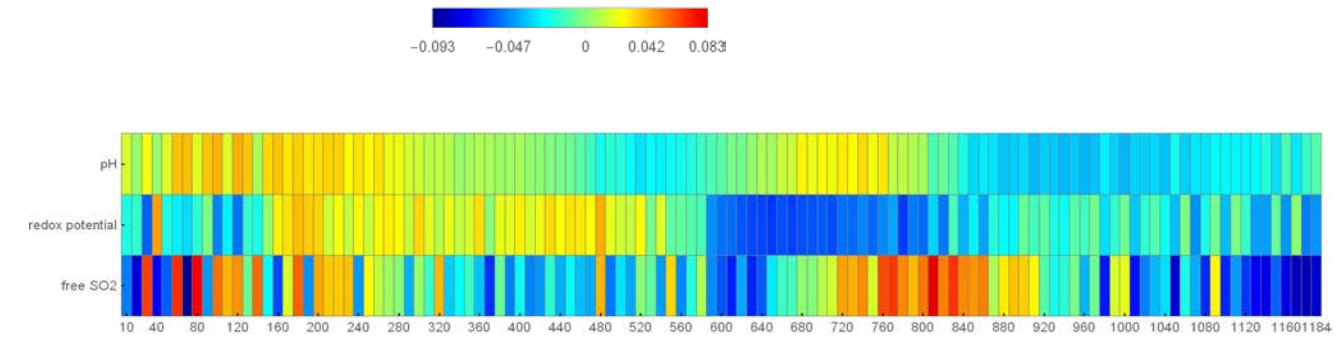

b)

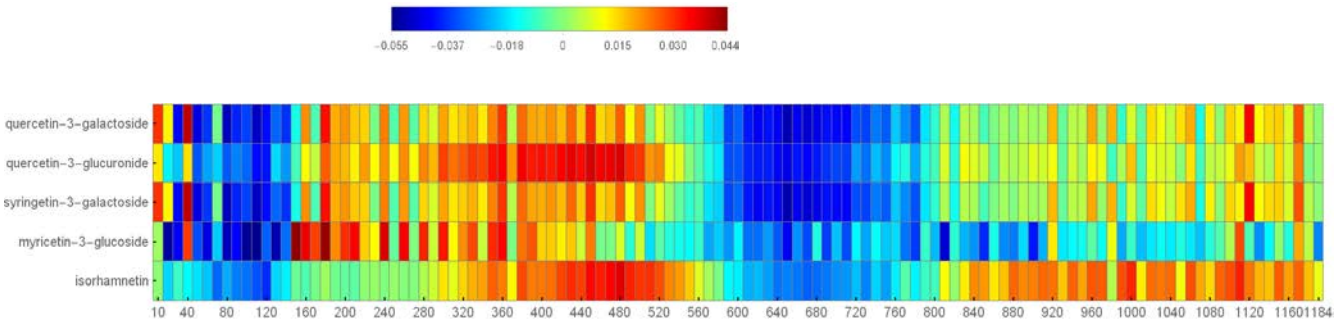

c)

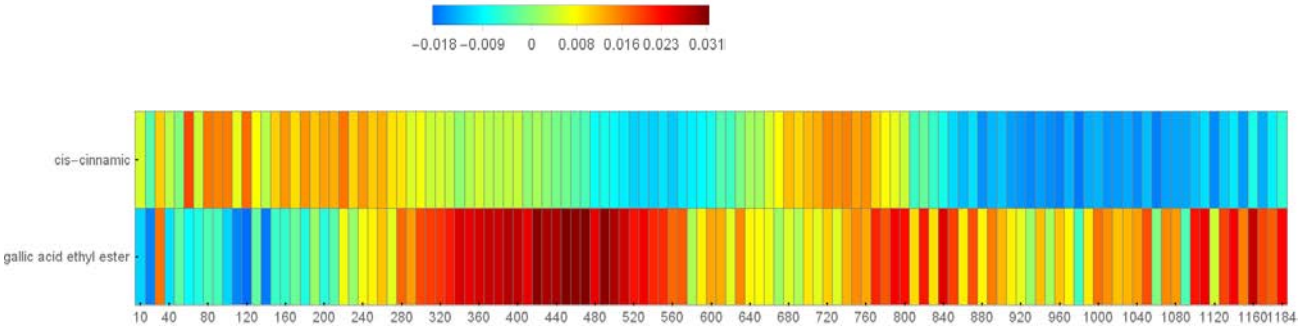

d)

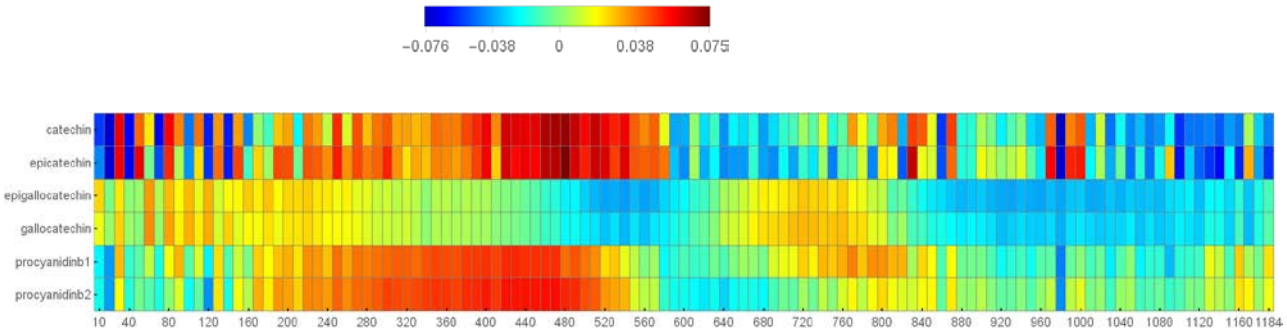

e)

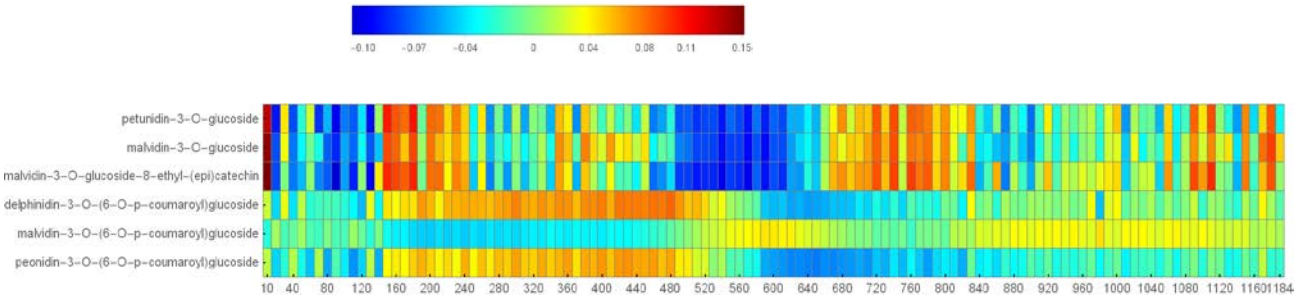
-0.10 -0.07 -0.04 0 0.04 0.08 0.11 0.15
petunidin-3-O-glucoside
malvidin-3-O-glucoside
malvidin-3-O-glucoside-8-ethyl-(epi)catechin
delphinidin-3-O-(6-O-p-coumaroyl)glucoside
malvidin-3-O-(6-O-p-coumaroyl)glucoside
peonidin-3-O-(6-O-p-coumaroyl)glucoside
10 40 80 120 160 200 240 280 320 360 400 440 480 520 560 600 640 680 720 760 800 840 880 920 960 1000 1040 1080 1120 1160 1184

f)

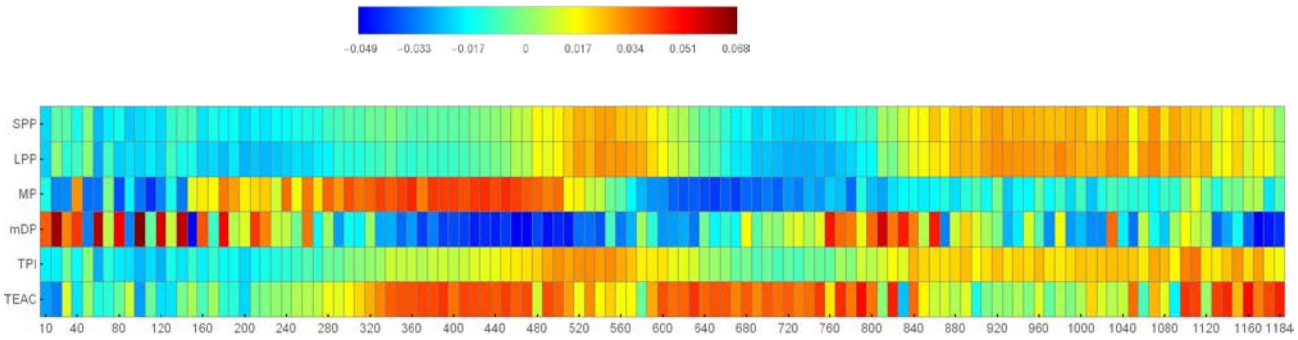
-0.049 -0.033 -0.017 0 0.017 0.034 0.051 0.068
SPP
LPP
MP
mDP
TPI
TEAC
10 40 80 120 160 200 240 280 320 360 400 440 480 520 560 600 640 680 720 760 800 840 880 920 960 1000 1040 1080 1120 1160 1184

g)

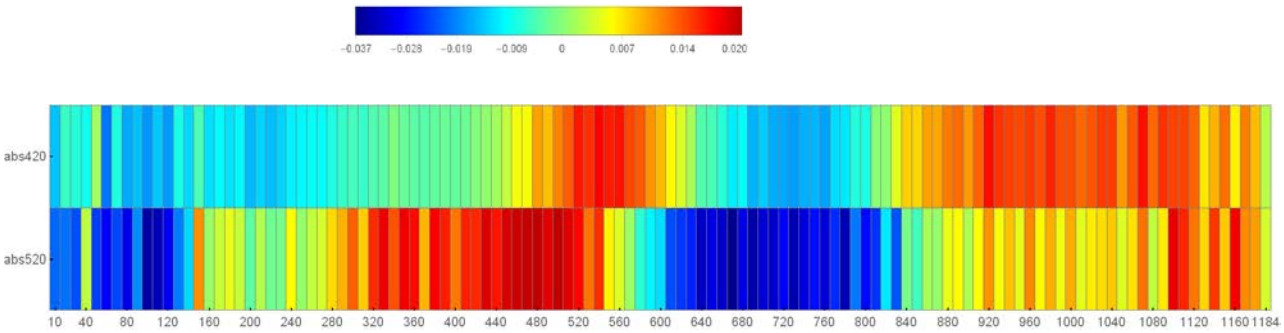
-0.037 -0.028 -0.019 -0.009 0 0.007 0.014 0.020
abs420
abs520
10 40 80 120 160 200 240 280 320 360 400 440 480 520 560 600 640 680 720 760 800 840 880 920 960 1000 1040 1080 1120 1160 1184

Figure 4

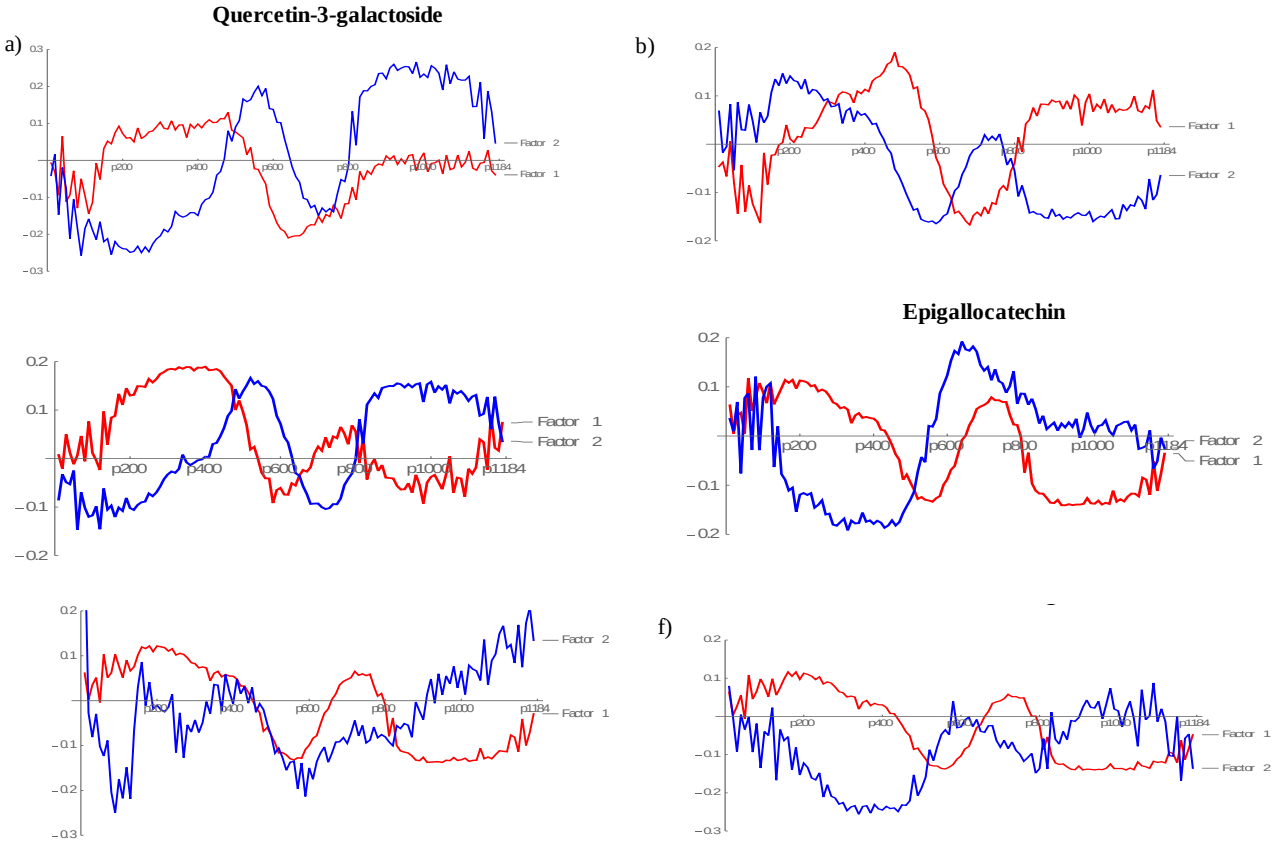
Quercetin-3-galactoside
a)
b)
Epigallocatechin
f)
Factor 1
Factor 2
p200
p400
p600
p800
p1000
p1184